Evaluation of the c_v -Measurements on the Critical Isochore of SF_6 Performed During the German Spacelab Mission D-2[1]

A. Haupt[2], J. Straub[3,4]

---

[1] Paper presented at the Thirteenth Symposium on Thermophysical Properties, June 22-27, 1997, Boulder, Colorado, U.S.A.

[2] Pichler Engineering GmbH, Arabellastr. 21 D-81925 Munich, Germany

[3] Institute A for Thermodynamics, Technical University Munich, Boltzmannstr. 15, D-85748 Garching, Germany

[4] To whom correspondence should be addressed

ABSTRACT

The evaluation of the c_v- measurements on the critical isochore of SF_6 performed with the newly developed scanning-radiation-calorimeter during the German Spacelab Mission D-2 is presented. During cooling in the 1-phase region under μg-conditions the "piston effect" avoids significant temperature and density inhomogenities in the fluid. In the 2-phase region both phases are continuously subcooled into the metastable region by the "piston effect" causing a permanent nucleation of small droplets and bubbles, which keeps the system near its thermodynamic equilibrium. For the slowest cooling run of $dT_0/dt = -0.06\ K \cdot h^{-1}$ at T_c, the c_v-data are distorted by ramp rate effects only for $|(T-T_c)/T_c| < 3\ 10^{-6}$. Using a range shrinking procedure for the determination of the asymptotic region the simple power law is valid for $|(T-T_c)/T_c| < 1.6\ 10^{-4}$. For the fitting procedure the theoretical constraints $\alpha = \alpha'$ and $B = B'$ are applied. Fitting the data in the asymptotic region to the simple power law yields the exponent $\alpha = 0{,}1105^{+0.025}_{-0.027}$ and the amplitude ratio $A^-/A^+ = 1{,}919^{+0.24}_{-0.27}$, in good agreement with values of the renormalization group theory (RGT) and other experiments for the 3,1-universality class. The validity of the power law extended by the first Wegner correction is found to be $|(T-T_c)/T_c| < 1\ 10^{-3}$, giving similar values for the fitting parameters. Testing the two-scale-factor universality by combining the critical amplitude with the correlation length gives $R_x = 0.284 \pm 0.018$, in agreement with theoretical estimates and other experimental values for fluid systems.

KEY WORDS: critical phenomena; isochoric heat capacity; microgravity; sulfur hexafluoride.

1 INTRODUCTION

During the D2-Mission a scanning-radiation-calorimeter was employed to measure c_v of SF_6 on the critical isochore during heating and cooling runs. This instrument has especially been developed to meet the experimental requirements under microgravity (µg-) conditions. The cooling runs allowed undistorted c_v-measurements in the immediate vicinity of the critical point, where earth-bound experiments are influenced by the implicit effect of gravity.

The technique of using cooling runs for the c_v-measurement near the critical point resulted from the analysis of the experiments performed during the D1-mission. In these experiments, the effect of isentropic heating ("piston effect") caused significant temperature differences in the fluid due to the different isentropic temperature coefficients $(\delta T/\delta p)_s$ of both phases. Under 1g-conditions these inhomogenities are diminished mainly by the effect of buoyancy convection, the limiting factor of optimized c_v-measurements (cell height H = 1 mm, heating rate $dT_0/dt = 3.6\ mK \cdot h^{-1}$) is the implicit effect of gravity. Under µg-conditions, however, the effect of isentropic heating becomes dominant and leads to a decisive hysteresis of c_v-courses obtained by the comparison of heating and cooling runs.

Furthermore, during cooling the "piston effect" determines the fluid behavior, though here the effect of isentropic heating keeps the fluid near its thermodynamic equilibrium. Approaching the critical point the temperature and density inhomogenities caused by heat conduction during cooling are reduced by the increasing influence of the piston effect due to the increasing thermal expansion coefficient $(\delta\rho/\delta T)p$. During cooling into the 2-phase region both phases are subcooled continuously into the metastable region by the "piston effect". Here homogeneous nucleation occurs in both phases and bubbles in

the liquid phase and droplets in the gaseous phase are created constantly. This fine emulsion of bubbles and droplets provides a large surface and short paths for the heat and mass transport during the phase transition. Therefore the fluid is kept near its thermodynamic equilibrium resulting in an almost undistorted cv-measurement.

Due to the limited space available for this paper we refer to [1] and [2] for a more detailed explanation of these phenomena and further information about the experiments performed during the D2-Mission. In this paper we give only a short summary of the main topics of the c_v-measurement and present the results and discussion of the final evaluation. For details on the construction and operation of the scanning-radiation-calorimeter we refer to [3].

2 EXPERIMENTAL DETAILS

We used a spherical cell made of copper with a diameter of 19.2 mm, produced in an electrolytic coating process. The cell is equipped with 4 thermistors, 1 on the wall and 3 at different radii inside the cell to measure the temperature distribution in the fluid.

The sample cell (stage 0) is heated and cooled passively through heat exchange with the surrounding stage 1 mainly by radiation. About 10 % of the total heat exchange is carried out by heat conduction via the electrical connections between the cell and stage 1. The isochoric heat of the sample is determined by the energy balance of the cell leading to:

$$c_V(T) = \left(\frac{(T_0 - T_1) + P_T(T)}{R_{th,01}(T) \cdot \frac{dT_0}{dt}} - C_C \right) \cdot \frac{1}{m_{Fluid}} \tag{1}$$

The temperature difference T_0-T_1 is measured directly between a thermistor in stage 1 and the cell thermistors, the determination of the temperature course dT_0 /dt of the cell is based on the measurement of the temperature T_1 and the difference T_0-T_1:

(2) $$\frac{dT_0}{dt} = \frac{d(T_1 + T_0 - T_1)}{dt}$$

With a wall thickness of 0.35 mm the total (mechanical and thermal) compressibility of the cell is $6 \cdot 10^{-5}$ K^{-1} . The spherical cell provides an excellent ratio of the total heat capacity and that of the fluid of 77% at $T-T_c$ = -0.1 K and 66% at $T-T_c$ = +0.1 K respectively. The cell volume determined by several measurements is V_C = 3,7626 cm^3 ±0.24%. The sample mass is m_{Fluid} = 2.773 g ±0.22%, yielding a sample density of ρ = 737.2 $kg \cdot m^{-3}$ ±0.27%. The sample purity was determined by the manufacturer to be 99.998%, mainly CH_4, N_2, H_2O. The maximum leak rate of the cell measured by weighing the filled cell over several days was less than 0.024 $\% \cdot year^{-1}$.

The thermal resistance $R_{th,01}(T)$ was measured at several temperatures in a temperature region of 12 K around T_c . The standard deviation of the fit of these data to a cubic function was less than 0.02 %, the accuracy of $R_{th,01}(T)$ is 0.47%. The heating power of the thermistor P_T (T) considered in Eq. (1) is less than 1% for all ramp rates.

The heat capacity of the cell C_C was determined after emptying the cell to be C_C = 2.03 $J \cdot K^{-1}$ with a heating and a cooling run. The small temperature coefficient of copper is neglected in the evaluation, the estimated accuracy of C_C is 2%.

All thermistors were calibrated at 10 different temperature levels in the range of 15 K spanning T_c with two Pt-25 sensors, integrated in stage 1. These sensors are calibrated by the manufacturer Rosemount to 2 mK. To reduce the drift of the thermistors they were aged artificially yielding a stability of dT/dt < 0.5 $mK \cdot year^{-1}$. The resistance-temperature-curve of each thermistor was fitted with the Steinhart-Hart-Equation, the mean standard deviation between data and fit is less than 0.5 mK for the measurement of T_0-T_1 and 2.2 mK for T_1 respectively.

With that the accuracy of the c_v -data above T_c is calculated to be about 3-4.5% for the ramp rates dT_0 /dt = –0.4 and –0.06 $K \cdot h^{-1}$ respectively. Below T_c the accuracy is about 1.5-2.5% for dT_0 /dt = –0.4 and –0.06 $K \cdot h^{-1}$ respectively. The precision of the c_v-data used for the analysis is about 1% in the complete temperature region except for $|T-T_c| <$ 10 mK.

3 REGRESSION ANALYSIS AND DISCUSSION

To obtain the asymptotic behavior of the specific isochoric heat we used the simple power law for data fitting:

$$c_V = A^{-/+}|\tau|^{-\alpha} + B \tag{3}$$

Here A^-/A^+ are the amplitude values below and above the critical temperature T_c, τ is the reduced temperature ($T-T_c/T_c$), α the critical exponent and B the regular background term. Our analysis follows the predictions of scaling theory that the critical exponent α has the same value below and above T_c ($\alpha = \alpha'$). In accordance to the renormalization theory we applied the constraint B = B' and since the sample density proved to meet the critical density of SF_6 within 1% we applied the same critical temperature for the data above and below ($T_c^+ = T_c^-$). Therefore we did not treat the data above and below T_c separately but fitted both branches simultaneously.

Equations of the form as Eq. (3) are non-linear, non-analytic functions which have a strong correlation between the parameters. This means there are a lot of parameter sets describing the data almost equally well. This is elucidated by our analysis where a shift of the critical temperature of only 0.1 mK yield a change of the exponent value of about 4% without a significant change of the least square sum. To confirm the fitting procedure finds the global minimum of the least square sum X_v independent of the fitting algorithm

Eq. (3) is treated as a linear function by the following procedure. A number of fits is performed with fixed values of T_c and α for each fit. By the variation of both parameters with a certain grid size and within reasonable limits the smallest value of X_v of all fits indicates the best fit function for this data set.

3.1 Final Data File

The final data set includes data from several cooling runs performed under μg-conditions cleared up by the data which are distorted obviously by ramp rate effects. The results of heating runs were not included since c_v-data measured during heating runs are significantly influenced by ramp rate effects in a wide temperature region around T_c.

Fig. 1 shows that the c_v-data obtained by cooling under μg-conditions are distorted only in the immediate vicinity of the critical point in spite of the comparatively high ramp rates. It must be mentioned that the total mission time did not allow to realize smaller ramp rates over a wide temperature range. A double-logarithmic representation (see [1]) reveals that a ramp rate effect in the c_v-course of the slowest cooling run under μg-conditions is obvious only in the temperature region of $|(T-T_c)/T_c| < 3\cdot10^{-6}$. The c_v-data of a run with the ramp rate $dT_0/dt = -0.4$ K·h^{-1} have a significant distortion only between $-1\cdot10^{-5} < (T-T_c)/T_c < 2\cdot10^{-5}$. The comparison with c_v-measurements of pure fluids using a scanning-ratio-calorimeter elucidates the advantage of the cooling technique under μg-conditions. Even with heating rates of $dT_0/dt = 3.6$ mK·h^{-1} the c_v-data are typically distorted by ramp rate effects in a region of $|(T-T_c)/T_c| < 3.5\cdot10^{-5}$ ([4], [5], [6]).

The final data set includes more than 70.000 data points, mainly from the slowest runs, in a temperature region of -3.5 K $< T-T_c < 2.4$ K. Due to the decreasing ramp rate of the quasi-exponential runs both the data density and noise of data of the final data set increase with decreased distance from T_c.

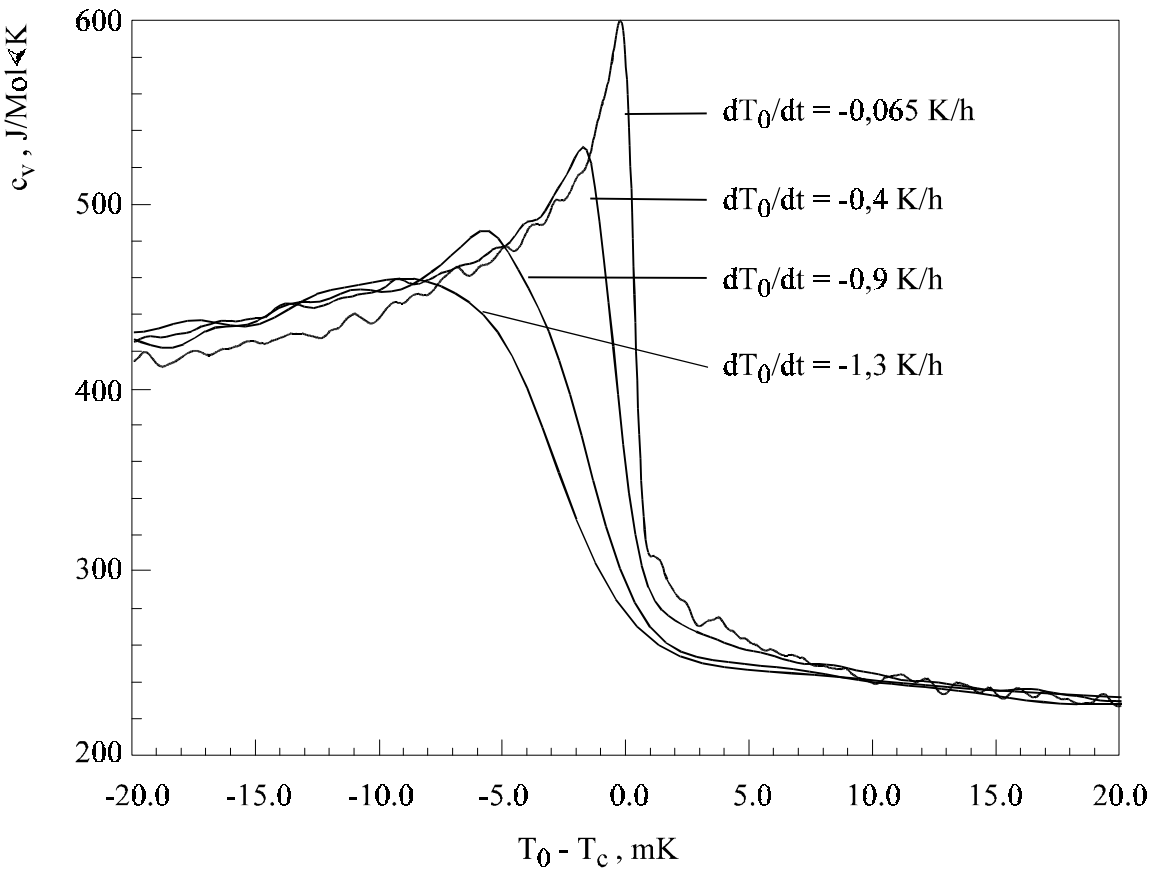

Fig. 1 Isochoric heat capacity c_v measured under μ*g*-conditions at different cooling rates. For comparison a c_v -course measured under 1*g*-conditions at a cooling rate of $dT_0/dt = -0{,}1\ K \cdot h^{-1}$ is given.

3.2 Data file averaging

For data file averaging we made use of the fact that in a double-logarithmic representation of c_v versus $\tau = (T-T_c)/T_c$ the c_v-slope is approximately linear. Each decade of τ is divided in j segments and for each segment the covered data are averaged to N_j data points ($c_{v,j}$, T_j). A reduced data set was created consisting of 2500 (c_v , T)-pairs which is available for further use by others (see Fig. 2). The different uncertainty of c_v-data obtained with different ramp rates was not considered resulting in a higher weighting of data obtained with the slow runs compared to those of the faster runs (see below). In

order to obtain a reasonable CPU-time for the regression analysis the 2500 pairs were reduced in the same manner to 40 data points per decade of τ.

The statistical uncertainty of the c_v-data depends mainly on the ramp rate and the distance from T_c since the cell temperature is not actively controlled but depends on c_v . In addition the unregular dynamics of the phase transition in the 2-phase region changes the noise of the data. Therefore it is not possible to assign a certain standard deviation to a certain run or a certain ramp rate.

Instead an individual uncertainty or rather a weighting factor for each data point is determined for the analysis concerning the asymptotic behavior of c_v. In addition the increasing temperature uncertainty of each data point approaching T_c is considered:

(4) $$\sigma_i^2 = \sigma_{c_v,i}^2 + \left|\frac{\partial c_{v,i}}{\partial T}\right|^2 \cdot \sigma_{T-T_c}^2$$

The individual uncertainties $\sigma_{cv,i}^2$ are obtained as the deviation between the c_v-data and a smoothing cubic spline applied to the c_v-data in logarithmic form. With that a bias effect on the individual uncertainties is avoided to the greatest possible extent since a smoothing spline represents the data without a functional dependency.

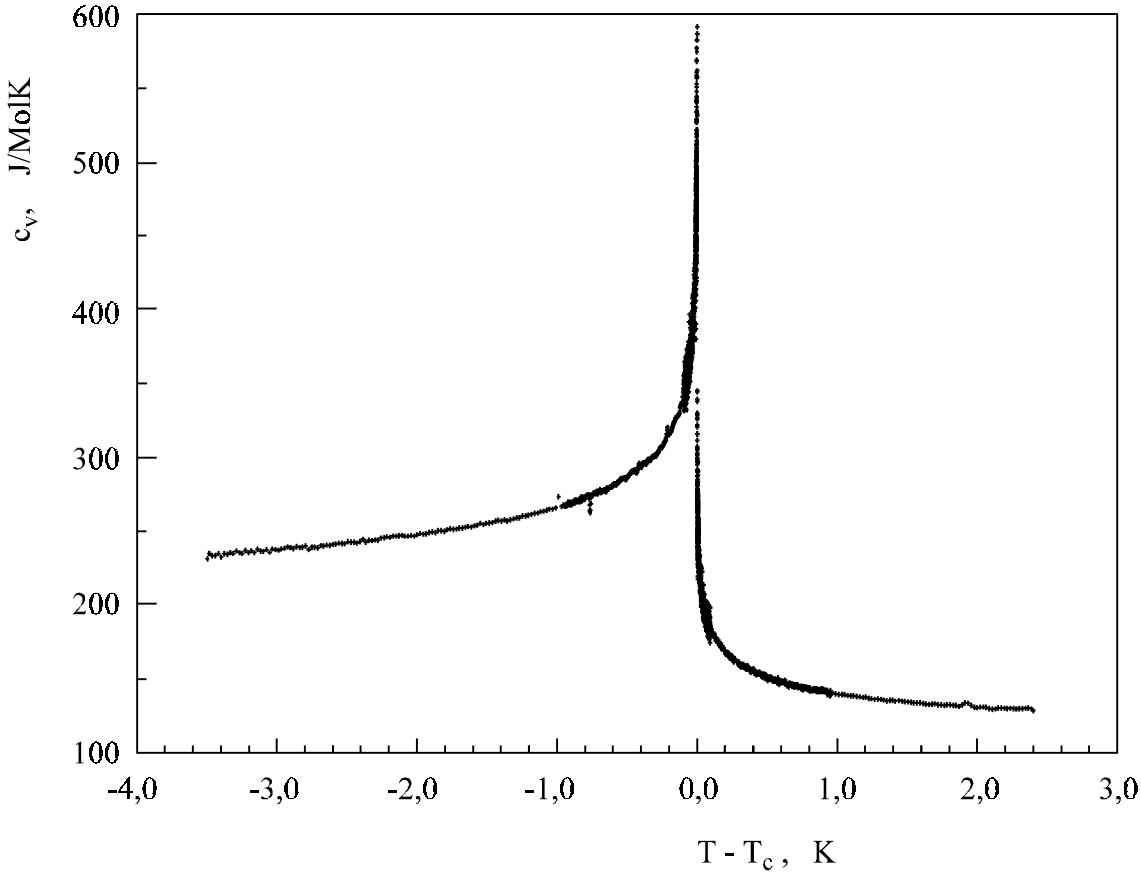

Fig. 2 Final c_v -data set consisting of 2500 (c_v , T-T_c)-pairs covering the temperature region –3.5 K < T-T_c < +2.4 K in a linear representation. This data set is available for use and further evaluation by others.

In addition smoothing the c_v-data in a logarithmic form provides the advantage that the increased noise when approaching T_c can be smoothed out by a "harder" spline without imposing a bias effect in that region where the c_v-course has the maximum increase. Especially near T_c a wrong estimation of the individual weighting factors would influence the result of the asymptotic analysis significantly. The spline parameter S, representing the weight of each data point for the spline fitting, must be chosen in the appropriate way. For higher values of S the smoothing spline change into an interpolating spline underestimating the real standard deviation of the data. On the contrary, too small values of S lead to a distorted representation of the c_v-course and weighting factors respectively.

In Eq. (4) the temperature uncertainty σ_{T-Tc} is estimated to be 500 μK, the factor ($\delta c_{v,i}/\delta T$) is taken from the smoothing spline. The weighting factors are determined with the data set consisting of 2500 points. For the again reduced data set used in the regression analysis the appropriate weighting factors where determined by averaging the individual factors in the same way as mentioned above.

3.3 Determination of the asymptotic region

A range shrinking method was used to determine the extension of the asymptotic region where the simple power law is valid for the description of c_v-data. For this task the critical temperature T_c used in the fitting procedure is a fixed parameter, for the determination of the best fit function in the asymptotic region T_c is used as a free parameter. From the c_v-course measured with the slowest cooling run ($dT_0/dt = -0.06$ K·h^{-1}) the critical temperature of the sample was found to be $T_c \approx 318.680$ K ± 0.5 mK.

The outer limit τ_{max} was varied between $6\cdot10^{-5} < \tau_{max} < 2\cdot10^{-3}$, the inner limit τ_{min} is fixed for all fits to $\tau_{min} = 3\cdot10^{-6}$. The largest fitting region includes 203 data points, the smallest region 81, 40 above and 41 below T_c. The range shrinking was realized by discarding a data point from above and below T_c after each fit.

Fig. 3 shows X_v^2-courses obtained by this method using four different values for the spline parameter S for the estimation of the weighting factors. It is obvious that X_v^2 reaches a nearly constant level between 1.05 and 1.2 for $|\tau_{max}| < 1.6\cdot10^{-4}$ independent of the value of S or rather the weighting factors used for fitting the data to the simple power law. A value of X_v^2 near unity stands for both a good estimation of the data uncertainties and a good suitability of the simple power law for describing the data in this temperature region.

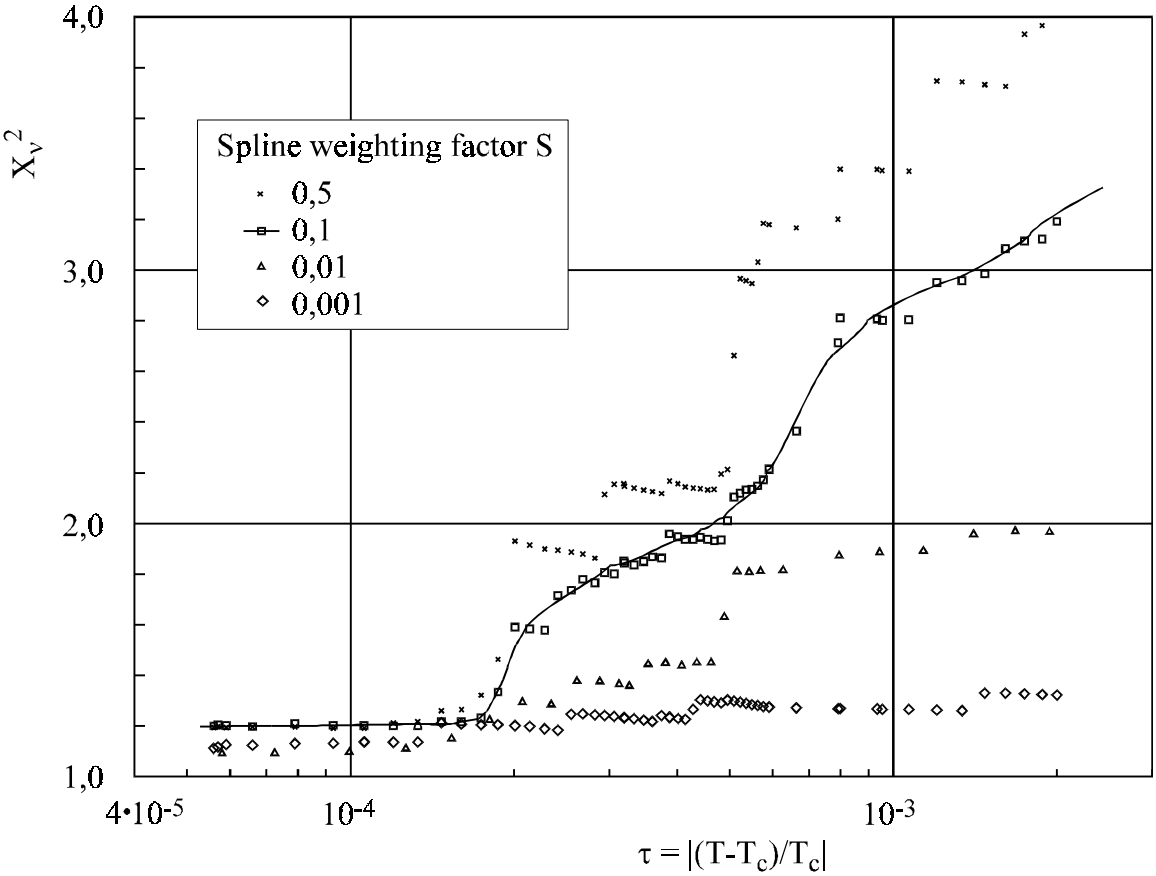

Fig. 3 Semi-log plot of the reduced chi-square X_v^2 as a function of the reduced temperature τ obtained by varying the fitting region („range-shrinking“) and the standard deviation of the data. The standard deviation of the final data set was determined by fitting the data by a smoothing cubic spline. To find the best estimate for the standard deviation of the data the spline parameter S was varied between 0.5 ("smooth" , nearly interpolating spline) and 0.001 ("hard" spline). Independent of the standard deviation used for fitting the data to the simple power law X_v^2 reaches a nearly constant value for $|\tau| < 1.6 \cdot 10^{-4}$ indicating the extension of the asymptotic region of the c_v-data.

As shown in Fig. 4 the fit parameters α, A^-/A^+ and B increase in a similar way when the outer limit τ_{max} is decreased and reach nearly constant values for $|\tau_{max}| < 1.6 \cdot 10^{-4}$, too. For these reasons the extension of the asymptotic region for our c_v -data of SF_6 is fixed to $|\tau| = 1.6 \cdot 10^{-4}$.

As shown in Fig. 3 for $\tau_{max} > 1.6 \cdot 10^{-4}$ X_v^2 increases for larger fitting regions depending on the value of S. The more S is increased the more X_v^2 goes up. Increasing the parameter S results in a decreased smoothing of the data resulting in an underestimation of the actual standard deviation. On the contrary decreasing S gives a „harder“ spline which tends to a systematic deviation between the spline and the c_v-course and a decreasing significance to find the asymptotic region. For these reasons the spline parameter S = 0.1 is chosen for the estimation of the individual uncertainties for the complete data set.

To find out any dependencies of the extension of the asymptotic region on the inner and outer limit of the data set the limits were varied between $3 \cdot 10^{-6} < |\tau_{min}| < 8 \cdot 10^{-6}$ and $1 \cdot 10^{-4} < |\tau_{max}| < 1.6 \cdot 10^{-4}$ respectively. The values of α and the amplitude ratio show an insignificant range of only 1% when τ_{min} is varied, the dependency on τ_{max} is about 2-4 % verifying an appropriate determination of the asymptotic region.

In comparison, c_v-measurements of CO_2 [4] yield an extension of the asymptotic region of $|\tau| = 4.5 \cdot 10^{-4}$, c_p-measurements of a binary mixture [7] result in $|\tau| = 6 \cdot 10^{-4}$. We assume that this small difference is due to the different procedures estimating the standard deviation of the data and the criterion applied to the determination of the asymptotic region.

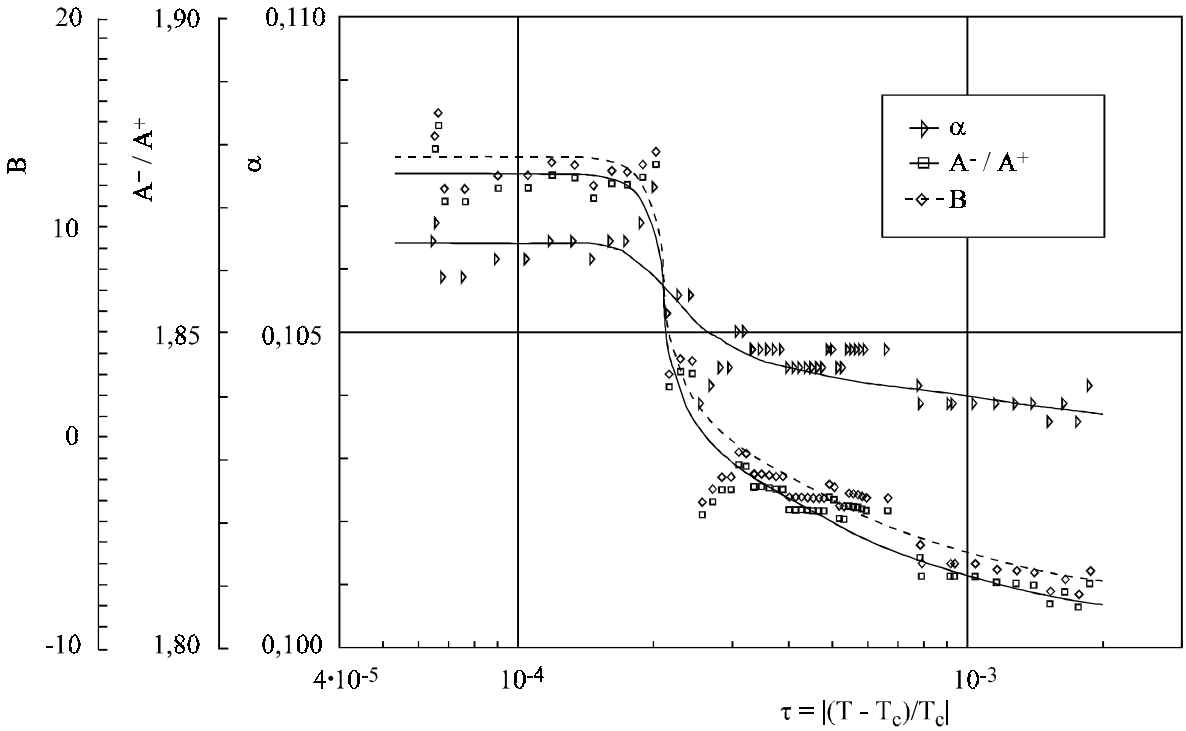

Fig. 4 Semi-log plot of the parameters α, A^-/A^+ and B as a function of the reduced temperature τ obtained by varying the fitting region ("range-shrinking"). The plotted courses were obtained with S = 0.1, the results for other values of S are in principle the same. Independent of the standard deviation used for fitting the data to the simple power law all parameters reach a nearly constant value for $|\tau| < 1.6 \cdot 10^{-4}$ indicating the extension of the asymptotic region of the c_v-data.

3.4 Analysis in the asymptotic region

The data set between $3 \cdot 10^{-6} < |\tau| < 1.6 \cdot 10^{-4}$ consists of 113 data points, T_c is now treated as a free parameter between 318.678 K and 318.682 K with an interval of 0.05 mK. To determine the best fit parameter α is varied as mentioned above between 0.06 and 0.15 with an interval of 0.0001. This analysis containing 7200 fits yields the critical temperature to T_c = 318.6801 K, 0.1 mK higher than the fixed value used above. The best fit parameters for the asymptotic region are:

$$\alpha = 0{,}1105 \pm 0{,}004$$

$$A^+ = 69{,}43 \pm 0{,}06 \text{ J/Mol·K}$$

$$A^- = 133{,}2 \pm 0{,}07 \text{ J/Mol·K}$$

$$B = 19{,}92 \pm 0{,}20 \text{ J/Mol·K}$$

$$A^-/A^+ = 1{,}919$$

with $X_\nu^2 = 1.135$ as the global minimum. The uncertainties given for the parameter represent the diagonal elements of the error matrix. They do not represent the absolute error since they depend on the statistical uncertainty of the data used in the analysis. A more realistic estimation of the uncertainties is given by the determination of the confidence level of the estimated parameter (see i.e. [8]). We determined the range of parameters which meet

$$\frac{X_\nu^2 - X_{\nu,0}^2}{X_{\nu,0}^2} \leq F(p, N - p)\,. \tag{5}$$

X_ν^2 is the reduced square sum of a certain parameter set, $X_{\nu,0}^2$ is the global minimum value of the best fit function. For the degree of freedom $N - p = 109$ (N number of data points in the asymptotic region, p number of parameters of the simple power law) the 5% F-distribution parameter is $F_{0.05} = 2.46$ and the 1% F-distribution parameter is $F_{0.01} = 3.50$.

Fig. 5 shows two projections of constant X_ν^2 into the α-T_c-parameter space representing the 95% and 99% confidence level of the best fit parameters above. The plot means a 95% (99%) probability that the real parameter values are within these contours. In the plot the global minimum ($X_\nu^2 = 1.135$) with T_c as a free parameter is given and the local minimum ($X_\nu^2 = 1.197$) with the critical temperature fixed to $T_c = 318.680$ K. This analysis yields the following estimation for the uncertainties of the exponent α, the amplitude ratio A^-/A^+ and the regular background term B:

$$\alpha = 0.1105^{+0.025}_{-0.027}$$

$$A^{-}/A^{+} = 1.919^{+0.24}_{-0.27}$$

$$B = 19.92^{+22.3}_{-26.5}\ \mathrm{J/Mol{\cdot}K}$$

The plot reveals the strong correlation between the critical exponent and the critical temperature. The slight change from the fixed value of T_c to the value found in the analysis with T_c as a free parameter of only 0.1 mK causes a change in α of 4 %!

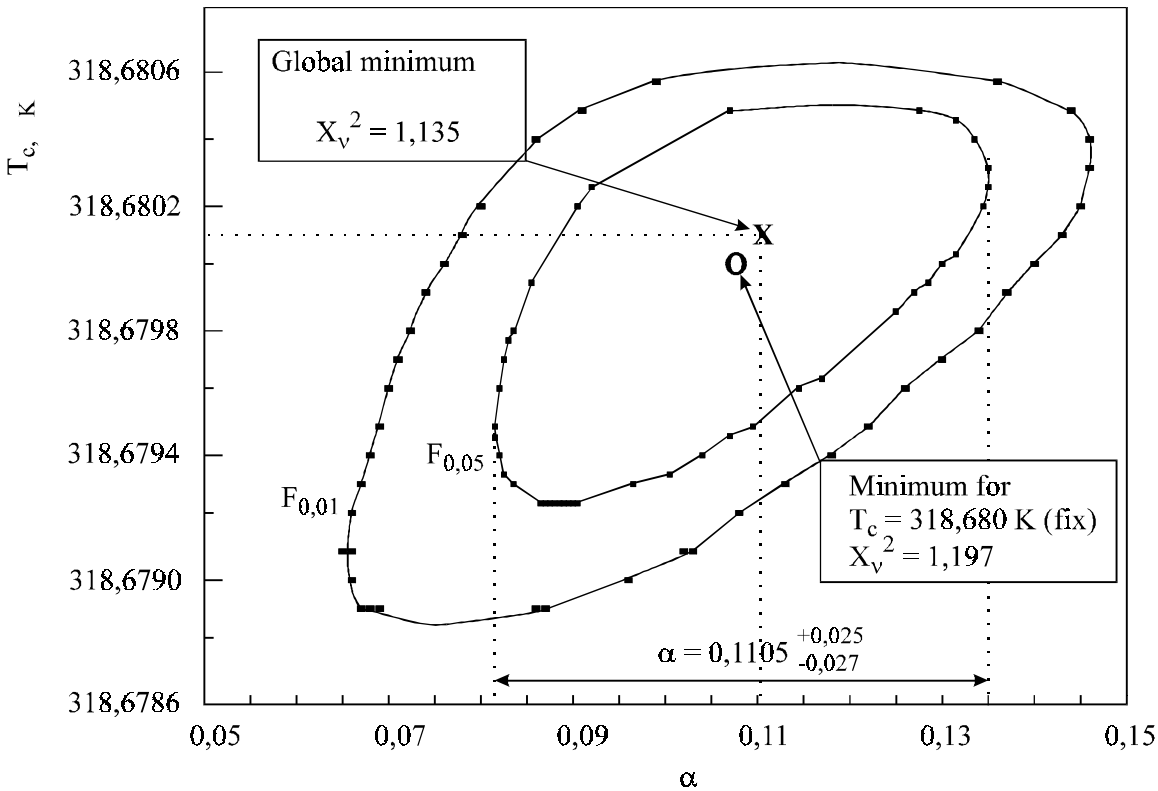

Fig. 5 Contours of constant X_ν^2 in the T_c-α parameter space representing the 95 % ($F_{0.05}$) and 99 % ($F_{0.01}$) confidence level for the values of α and T_c determined in the asymptotic region. The global minimum of the fit with T_c as a free parameter is marked by X (T_c is found to be 318.6801 K), the local minimum obtained with T_c fixed to 318.680 K is marked by O.

Fig. 6 shows the deviations of the reduced data set from the best fit parameters determined in the asymptotic region. The absence of any unbalanced deviations for both the

data below and above T_c verifies again the best fit function to be a good representation of the experimental data in the asymptotic region. The increasing systematic deviations of both courses from the best fit function beyond $|\tau| = 1.6 \cdot 10^{-4}$ elucidate that the simple power law must be extended by additional terms outside the asymptotic region.

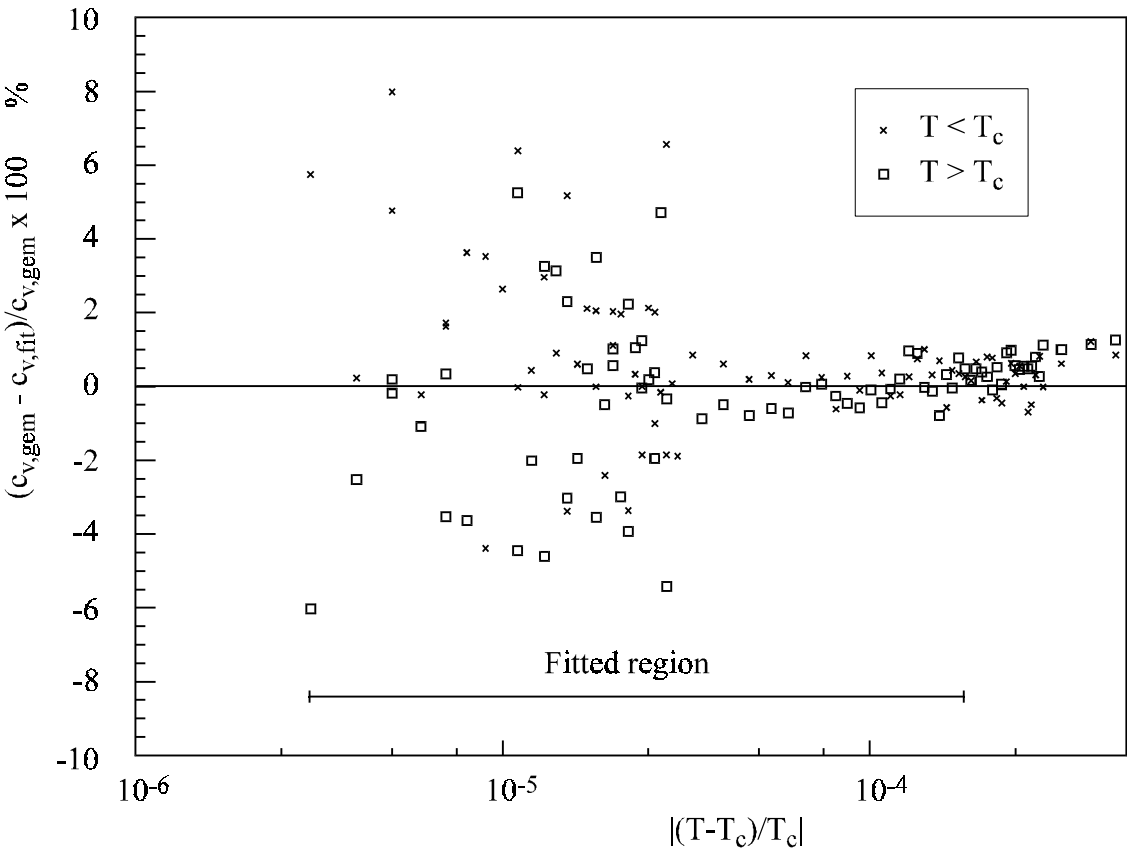

Fig. 6 Deviations of the reduced data set from the best fit function in the asymptotic region measured in percentage units. Beyond the asymptotic region both the c_v-data for $T<T_c$ (marked by x) and $T>T_c$ (marked by) show a significant increase of the deviation to the best fit function of the asymptotic region.

3.5 Analysis beyond the asymptotic region

To describe the data beyond the asymptotic region the simple power law is extended by the 1. Wegner correction [9]:

(6) $$c_V = A^{-/+}|\tau|^{-\alpha}\left(1 + D^{-/+}|\tau|^{\Delta}\right) + B$$

The temperature region where this model is a good representation of the data is determined with a range shrinking method as used for the asymptotic region. For this analysis the exponent Δ is set to the theoretical value 0.5 [10], the critical temperature is fixed to T_c = 318.680 K, the other parameters of Eq. (6) are treated as free parameters. The inner limit is fixed again at $|\tau_{min}| = 3\cdot10^{-6}$, the outer limit is varied between $4\cdot10^{-4} < |\tau_{max}| < 1\cdot10^{-2}$. After each fit the data set fitted is reduced by discarding a data point from above and below T_c. The analysis yields a monotonically decreasing X_v^2 until $|\tau_{max}| = 1.0\cdot10^{-3}$, in the temperature region $|\tau_{max}| < 1.0\cdot10^{-3}$ the reduced chi-square reaches a nearly constant course at $X_v^2 \approx 1.2$. This indicates both a good estimation of the standard deviation and a good suitability of the extended model for describing the data in this temperature region.

To find the best fit function of Eq. (6) for $|\tau_{max}| < 1.0\cdot10^{-3}$ the amount of 175 points in this temperature region is fitted by varying α from 0.08 to 0.13 (step 0.0001) and T_c between 318.679 K and 318.681 K (step 0.1 mK), the exponent Δ is fixed to 0.5. The analysis yields X_v^2 = 1.189 and the critical temperature T_c = 318.6802 K, only 0.1 mK higher than the value determined in the asymptotic region. The value of the critical exponent shows only a small change compared to the best fit function in the asymptotic region to $\alpha = 0.1115^{+0.045}_{-0.035}$. The parameter A^-, A^+ and B show a distinct shift of about 10%, the amplitude ratio yields to be $A^-/A^+ = 2.01^{+0.32}_{-0.40}$, clearly within the 95% confidence level of the value in the asymptotic region. The estimated uncertainties given for the exponent and the amplitude ratio represent the 95 % confidence level for the best fit function. The increased degree of freedom when fitting the data to Eq. (6) results inevi-

tably in an increased uncertainty of the best fit function compared to the uncertainties of the best fit function of Eq. (3).

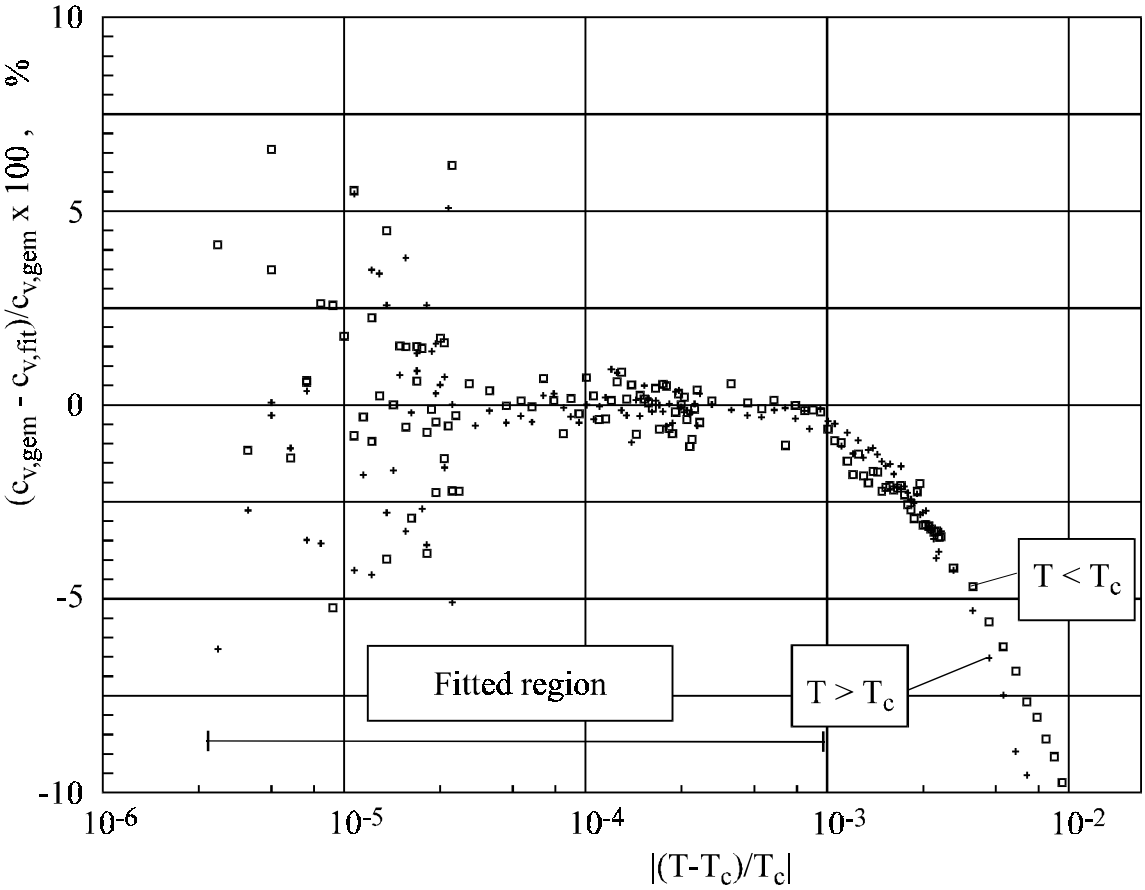

Fig. 7 Deviations of the reduced data set from the best fit function using the first Wegner correction. For $|\tau| > 1 \cdot 10^{-3}$ both the c_v-data for $T<T_c$ (marked by) and $T>T_c$ (marked by +) show a significant increase of the deviation to the best fit function of this region.

Fig. 7 shows the deviations of the complete data set from the best fit function in the temperature region mentioned above. The plot verifies that the asymptotic power law extended by the first Wegner correction is a good representation of the data set for $|\tau_{max}| < 1.0 \cdot 10^{-3}$. For larger temperature regions the plot clearly reveals increasing deviations for both the c_v-course above and below T_c .

To describe the data beyond $|\tau| > 1.0 \cdot 10^{-3}$ Eq. (6) was extended by the second Wegner correction:

$$c_V = A^{-/+}|\tau|^{-\alpha}\left(1 + D^{-/+}|\tau|^{\Delta} + E^{-/+}|\tau|^{2\Delta}\right) + B \tag{7}$$

The complete data set of 254 data points which covers a temperature region of about $|\tau| = 2 \cdot 10^{-2}$ was fitted to this function with the critical temperature fixed to $T_c = 318.6801$K and the exponent Δ fixed to the theoretical value 0.5. The other parameters of Eq. (7) were treated as free parameters, the analysis was performed by varying the critical exponent between $0.08 < \alpha < 0.13$ with a step of $\Delta\alpha = 0.0001$. The analysis yields slightly changed parameter values but a relative high value of the reduced chi square of $X_\nu^2 = 2.14$ indicates that Eq. (7) is an insufficient representation of the complete data set. This is confirmed by Fig. 8 which represents the deviations between the complete data set and the best fit function in the complete temperature region. The c_v-data in the 2-phase region below $\tau < -2 \cdot 10^{-3}$ show a significant deviation from the best fit function, in the contrary, the deviation of the 1-phase data do not increase 1% for the complete temperature region.

In addition instead of Eq. (7) the following model used by [5] and [7] was applied to the analysis of the complete data set:

$$c_V = A^{-/+}|\tau|^{-\alpha}\left(1 + D^{-/+}|\tau|^{\Delta}\right) + E^{-/+}|\tau|^{2\Delta} + B \tag{8}$$

The higher value of $X_\nu^2 = 2.26$ indicates that this is a worse representation of the complete data set than Eq. (7).

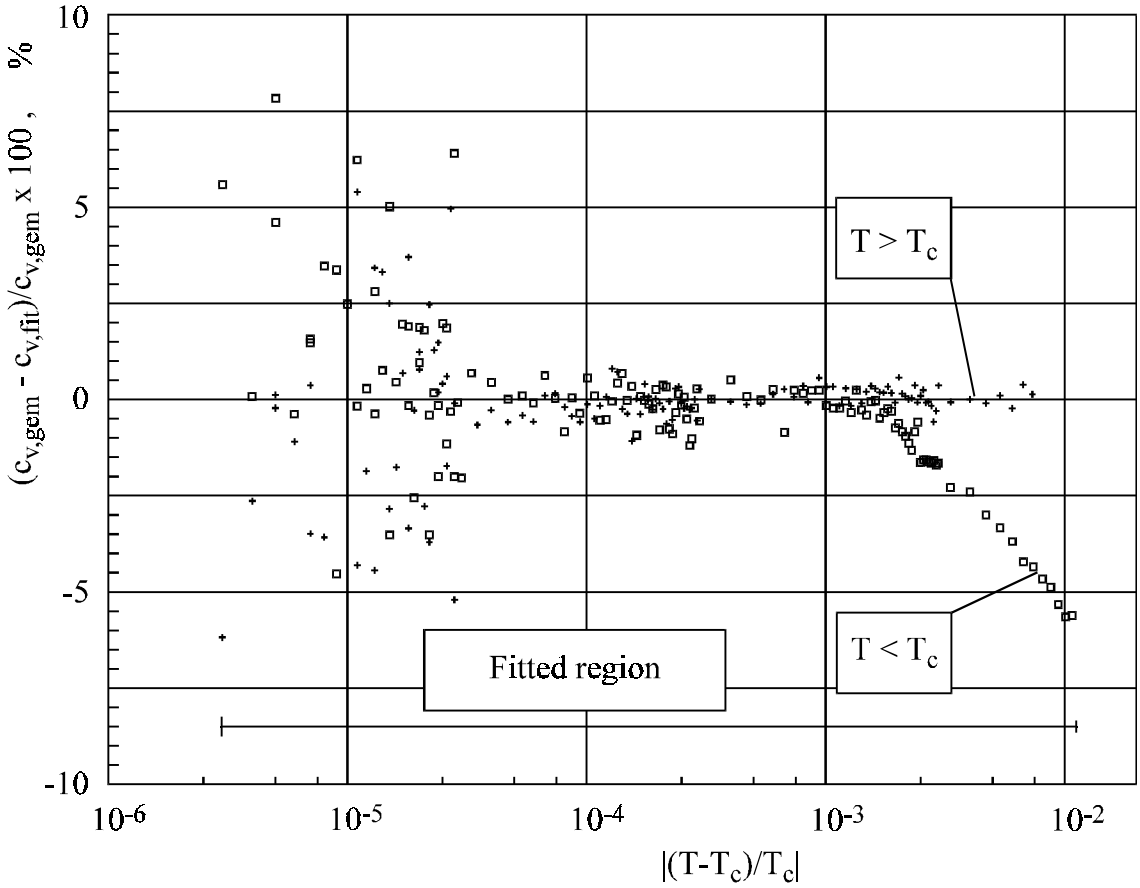

Fig. 8 Deviations of the reduced data set from the best fit function using the second Wegner correction. For $\tau > 2 \cdot 10^{-3}$ the c_v-data for $T<T_c$ (marked by) show a significant increase of the deviation to the best fit function of this region. In contrast the deviations of c_v-data above T_c (marked by +) are below 1% indicating a good representation by the model.

With this analysis it is not clear whether the reason for the observed deviations between our c_v-data and the model extended by the second Wegner correction lies in our c_v-data or in the model. The analysis of high-precision measurements of the isochoric heat of CO_2 by [4] yielded a good suitability of Eq. (7) in a temperature region of $-5 \cdot 10^{-2} < \tau < 2{,}7 \cdot 10^{-2}$. Though a view on our c_v-data of does not show any significant misbehavior in this region. A bias effect due to the average procedure has to be excluded since the analysis of the original data set shows the same deviation in this temperature region.

3.6 Two scale factor universality

To check the validity of hyperscaling the parameters of the best fit function valid for the asymptotic region were combined with the correlation length for SF_6. The universal factor was determined with

$$R_\xi = \xi_0 \left(\frac{\alpha \cdot A^+ \cdot \rho_c \cdot R}{k_B} \right)^{\frac{1}{d}} \tag{9}$$

resulting in $R_\xi = 0.284 \pm 0.018$ with $\xi_0 = 2.016 \cdot 10^{-10}$ m [11], R=56.92 $J \cdot g^{-1} K^{-1}$, ρ_c as the sample density, k_B the Boltzmann constant and d =3. As shown in Table 1 this value is in good agreement with experiments on other 3,1-systems and theoretical calculations.

3.7 Comparison with other experiments and theory

The statistical analysis in the asymptotic region yields the critical temperature of the sample to be T_c = 318.6801 K, the estimated uncertainty with 95 % confidence level is +0.4/–0.9 mK (see Fig. 5). The accuracy of the temperature measurement was calibrated to be ±10 mK. This value matches the position of the c_v-singularity measured with the slowest cooling run within a few 1/10 mK. However, the value is about 50 mK below the values of experiments using high quality samples. For a 5.4-SF_6 (purity 99.9994 %) the measurement of [12] yields T_c = 318.730 K and ρ_c = 742.1 $kg \cdot m^{-3}$, for a 5.5-SF_6 the measurements of [13] and [14] results in T_c = 318.736 K, ρ_c = 738.8 $kg \cdot m^{-3}$ and T_c = 318.723 K, ρ_c = 734.4 $kg \cdot m^{-3}$ respectively. The comparison of the measured T_c and the quality of the sample fluid for several experiments in the literature shows that T_c decreases with decreasing quality since the impurities are mainly O_2, N_2, CH_4. Since the density of our sample matches the critical density of SF_6 within 1% the difference in T_c is caused only by impurities. According to the analysis mentioned above the critical temperature of our sample indicates that the quality of our sample is better than 3.8. The

original quality measured by the fluid manufacturer was 4.8. We suspect that the additional impurities come from the fact that the cell could not be evacuated at high temperatures before the filling due to the soft soldered thermistors in the cell.

Several investigations reveal that the behavior of the critical exponent α do not change significantly even for impurities of a few percent of the sample volume ([6], [15]). Therefore an influence of the small amount of impurities (< 0.02 %) in our sample on the universal parameters can be definitely excluded.

Table 1 gives a comparison of curve fitting in the asymptotic region between this work and other experiments and the results of theoretical calculations. It is shown that the values of the critical exponent α and the universal amplitude ratio A/A^+ determined in the asymptotic region are in good agreement both with other experiments and theoretical results for 3,1-systems. The extension of the asymptotic region determined in this work is smaller compared to other experiments. At first glance the estimated uncertainties of α and A/A^+ of this work seem to be rather high compared to the results of the other experiments, which give uncertainties of about 2 to 5 % for the critical parameters. This difference is caused by the following reasons: First it has to be considered which method is used to estimate the statistical uncertainties. The diagonal elements of the error matrix normally yields smaller uncertainties than the determination by the confidence level. The first method is i.e. used by [5], [7] and [16]. Secondly the estimated uncertainty depends on the extension of the region fitted by the simple power law. The larger the fitting region the more data with a smaller standard deviation are included in the fit resulting in a smaller uncertainty of the fit parameter. As mentioned above the uncertainties depend on the strong correlation between the fitting parameters (see Fig. 5). Edwards [4] determines the critical temperature of the sample by independent time constant measurements

with an uncertainty of only ±0.15 mK! Therefore Edwards can reduce the estimated uncertainty determined by the confidence level method of about 10% to the values shown in Table 1.

A more precise determination of T_c in this work would have been possible only by much smaller ramp rates reducing the rounding of the c_v-singularity when passing the critical point. However, the slowest ramp rates realized during the D2-Mission made use both of the technical limits of the apparatus and the time resources of a Spacelab Mission.

ACKNOWLEDGMENTS

This research is supported by Deutsche Agentur für Raumfahrtangelegenheiten (DARA), project number 50 QV 8948. The authors are very grateful to all persons who contributed with their work to the success of the D2 experiment HPT-HYDRA. In particular we want to thank the crew of the Space Shuttle Columbia STS 55, the responsible persons of the company Kayser-Threde, Munich, the operations control team of DLR and NASA and all colleagues and students for their outstanding engagement.

Table 1: Comparison of the curve fitting in the asymptotic region of this work to other experiments and to theoretical calculations of the critical parameters. References of the theoretical values are: a) [18], b) [19], c) [20], d) [21], e) [22], f) [23], g) [24], h) [25], i) [26].

System	**Model**	**fitting region**	**α**	**A^-/A^+**	**R_ξ**	**Reference**
SF_6	$c_v = A^{+/-}\lvert\tau\rvert^{-\alpha} + B$	$3\cdot10^{-6} < \lvert\tau\rvert < 1{,}6\cdot10^{-4}$	0,1105 –0,027/+0,025	1,919–0,27/+0,24	0,284 ± 0,018	this work
SF_6	$c_v = A^{+/-}\lvert\tau\rvert^{-\alpha} + B$	$3{,}5\cdot10^{-5} < \lvert\tau\rvert < 2\cdot10^{-3}$	0,098 ± 0,01	1,83± 0,02	0,273	[5]
SF_6	$c_v = A^{+/-}\lvert\tau\rvert^{-\alpha} + B$	$5\cdot10^{-5} < \lvert\tau\rvert < 1{,}6\cdot10^{-3}$	0,1075 ±0,0054	1,86± 0,06	0,263	[16]
CO_2	$c_v = A^{+/-}\lvert\tau\rvert^{-\alpha} + B^{+/-}$	$4\cdot10^{-5} < \lvert\tau\rvert < 5\cdot10^{-3}$	0,124 ± 0,005	1,86± 0,06		[6]
CO_2	$c_v = A^{+/-}\lvert\tau\rvert^{-\alpha} + B$	$4\cdot10^{-5} < \lvert\tau\rvert < 5\cdot10^{-3}$	0,105	1,90		[17]
CO_2	$c_v = A^{+/-}\lvert\tau\rvert^{-\alpha} + B$	$4\cdot10^{-5} < \lvert\tau\rvert < 4{,}5\cdot10^{-4}$	0,1084 ±0,0023	1,965± 0,03	0,259 ± 0,016	[4]
3EA-D_2O	$c_v = A^{+/-}\lvert\tau\rvert^{-\alpha} + B$	$7\cdot10^{-6} < \lvert\tau\rvert < 6{,}0\cdot10^{-4}$	0,107 ± 0,002	1,75± 0,03	0,26 ± 0,03	[7]
HTS			0,112± 0,008[a)]	1,96[b)]	0,2547 ± 0,007[c)]	see labeling
RGT 3,1 System			0,110 ± 0,005[d)] 0,1094±0,0009[e)]	1,82-2,08[f)g)h)]	0,2699 ±0,0008[b)i)]	see labeling

REFERENCES

[1] J. Straub, A. Haupt and L. Eicher, Int. J. Thermophys. **16**: 1033 (1995).

[2] J. Straub, L. Eicher, and A. Haupt, Phys. Rev. E **51**: 5556 (1995).

[3] J. Straub, A. Haupt, and K. Nitsche, Fluid Phase Equilibria **88:** 123 (1993).

[4] T.J. Edwards, *Specific Heat Measurements near the Critical Point of* CO_2, Thesis, University of Western Australia (1984).

[5] R. Lange, *Die isochore Wärmekapazität fluider Stoffe im kritischen Gebiet*, Thesis, Technical University of Munich, Germany (1984).

[6] J.A. Lipa, C. Edwards, and Buckingham, Phys. Rev. A **15**: 778 (1977).

[7] E. Bloemen, J. Thoen, and W. Van Dael, J. Chem. Phys. **73**: 4628 (1980).

[8] Ph.R. Bevington and K. Robinson, *Data reduction and error analysis for the physical sciences*, ed. (McGraw - Hill, New York 1991)

[9] T. Wegner, Phys. Rev. B **5**: 4529 (1972).

[10] M. Barmatz, P.G. Hohenberg and A. Kornblit, Phys. Rev. B **12**: 1947 (1975).

[11] D.S. Cannel, Phys. Rev. A **6**: 225 (1975).

[12] W. Wagner, N. Kurzeja and B. Pieperbeck, Fluid Phase Equilibria **79**: 151(1992).

[13] D.Y. Ivanov, L.A. Makarevich, and O.N. Sokolova, Zhurnal Eksperimental ´noj i Teoreticeskoj Fiziki **20**: 272 (1974)

[14] L.A. Makarevich, O.N. Sokolova and A.M. Rozen, Sov. Phys. JETP **40**: 305 (1975)

[15] A.V. Voronel in *Phase Transitions and Critical Phenomena*: *Thermal Measurements and Critical Phenomena in Liquids,* Vol. 5B, C. Domb and M.S. Green, ed. (Academic Press, London, 1976), p. 343.

[16] J. Straub and K. Nitsche, Fluid Phase Equilibria **88**: 183 (1993)

[17] M.R. Moldover in *Phase Transitions: Cargese 1980*, ed. M. Levy, J.C. Le Guillou, J. Zinn-Justin (Plenum, New York, 1982), p. 62.

[18] B.G. Nickel in *Phase Transitions: Cargese 1980*, ed. M. Levy, J.C. Le Guillou, J. Zinn-Justin (Plenum, New York, 1982)

[19] P.C Hohenberg and A. Aharony, et al., Phys. Rev. B **13**: 2986 (1976)

[20] D. Stauffer, M. Ferer and M. Woritz, Phys. Rev. Lett. **29**: 345 (1972).

[21] J.C. Le Guillou and J. Zinn-Justin, Phys. Rev. B **21**: 3976 (1980)

[22] D.Z. Albert, Phys. Rev. B **25**: 4810 (1982)

[23] M. Barmatz and P.G. Hohenberg, A. Kornblit, Phys. Rev. B, **12**: 1947 (1975)

[24] A. Aharony and P.C. Hohenberg, (1976) Phys. Rev. B **13**: 3081 (1976)

[25] C. Bervillier, Phys. Rev. B **14**: 4964 (1976)

[26] C. Bervillier and C. Godreche, Phys. Rev. B **21**: 5427 (1980)